ISSN 1674-1056
http://cpb.iphy.ac.cn
http://iopscience.iop.org/cpb
中国物理 B
Chinese Physics
中国物理 Chinese Physics B

Shock-induced migration of asymmetry tilt grain boundary in iron bicrystal: A case study of Σ3[110]

Xueyang Zhang(张学阳)[1,2], Kun Wang(王昆)[2], Jun Chen(陈军)[2,3], Wangyu Hu(胡望宇)[4], Wenjun Zhu(祝文军)[5], Shifang Xiao(肖时芳)[1], Huiqiu Deng(邓辉球)[1], Mengqiu Cai(蔡孟秋)[1]

Citation: Chin. Phys. B . 2019, 28(12): 126201 . **doi:** 10.1088/1674-1056/ab4f61
Journal homepage: http://cpb.iphy.ac.cn; http://iopscience.iop.org/cpb

What follows is a list of articles you may be interested in

High-pressure electrides: From design to synthesis

Biao Wan(万彪), Jingwu Zhang(张静武), Lailei Wu(吴来磊), Huiyang Gou(缑慧阳)
Chin. Phys. B . 2019, 28(10): 106201 . **doi:** 10.1088/1674-1056/ab3f95

Transport properties of topological nodal-line semimetal candidate $CaAs_3$ under hydrostatic pressure

Jing Li(李婧), Ling-Xiao Zhao(赵凌霄), Yi-Yan Wang(王义炎), Xin-Min Wang(王欣敏), Chao-Yang Ma(麻朝阳), Wen-Liang Zhu(朱文亮), Mo-Ran Gao(高默然), Shuai Zhang(张帅), Zhi-An Ren(任治安), Gen-Fu Chen(陈根富)
Chin. Phys. B . 2019, 28(4): 046202 . **doi:** 10.1088/1674-1056/28/4/046202

Phase transitions in bismuth under rapid compression

Dong-Liang Yang(杨栋亮), Jing Liu(刘景), Chuan-Long Lin(林传龙), Qiu-Min Jing(敬秋民), Yi Zhang(张毅), Yu Gong(宫宇), Yan-Chun Li(李延春), Xiao-Dong Li(李晓东)
Chin. Phys. B . 2019, 28(3): 036201 . **doi:** 10.1088/1674-1056/28/3/036201

Shock temperature and reflectivity of precompressed H_2O up to 350 GPa:Approaching the interior of planets

Zhi-Yu He(贺芝宇), Hua Shu(舒桦), Xiu-Guang Huang(黄秀光), Qi-Li Zhang(张其黎), Guo Jia(贾果), Fan Zhang(张帆), Yu-Chun Tu(涂昱淳), Jun-Yue Wang(王寓越), Jun-Jian Ye(叶君建), Zhi-Yong Xie(谢志勇), Zhi-Heng Fang(方智恒), Wen-Bing Pei(裴文兵), Si-Zu Fu(傅思祖)
Chin. Phys. B . 2018, 27(12): 126202 . **doi:** 10.1088/1674-1056/27/12/126202

Unusual softening behavior of yield strength in niobium at high pressures

Qiu-Min Jing(敬秋民), Qiang He(何强), Yi Zhang(张毅), Shou-Rui Li(李守瑞), Lei Liu(柳雷), Qi-Yue Hou(侯琪玥), Hua-Yun Geng(耿华运), Yan Bi(毕延), Yu-Ying Yu(俞宇颖), Qiang Wu(吴强)
Chin. Phys. B . 2018, 27(10): 106201 . **doi:** 10.1088/1674-1056/27/10/106201

Shock-induced migration of asymmetry tilt grain boundary in iron bicrystal: A case study of Σ3 [110]*

Xueyang Zhang(张学阳)[1,2], Kun Wang(王昆)[2], Jun Chen(陈军)[2,3,†], Wangyu Hu(胡望宇)[4,‡], Wenjun Zhu(祝文军)[5], Shifang Xiao(肖时芳)[1], Huiqiu Deng(邓辉球)[1], and Mengqiu Cai(蔡孟秋)[1]

[1] *Department of Applied Physics, School of Physics and Electronics, Hunan University, Changsha* 410082, *China*
[2] *Laboratory of Computational Physics, Institute of Applied Physics and Computational Mathematics, Beijing* 100088, *China*
[3] *Center for Applied Physics and Technology, Peking University, Beijing* 100087, *China*
[4] *College of Materials Science and Engineering, Hunan University, Changsha* 410082, *China*
[5] *National Key Laboratory of Shock Wave and Detonation Physics, Institute of Fluid Physics, Mianyang* 621900, *China*

(Received 6 September 2019; revised manuscript received 17 October 2019; published online 15 November 2019)

Many of our previous studies have discussed the shock response of symmetrical grain boundaries in iron bicrystals. In this paper, the molecular dynamics simulation of an iron bicrystal containing Σ3 [110] asymmetry tilt grain boundary (ATGB) under shock-loading is performed. We find that the shock response of asymmetric grain boundaries is quite different from that of symmetric grain boundaries. Especially, our simulation proves that shock can induce migration of asymmetric grain boundary in iron. We also find that the shape and local structure of grain boundary (GB) would not be changed during shock-induced migration of Σ3 [110] ATGB, while the phase transformation near the GB could affect migration of GB. The most important discovery is that the shock-induced shear stress difference between two sides of GB is the key factor leading to GB migration. Our simulation involves a variety of piston velocities, and the migration of GB seems to be less sensitive to the piston velocity. Finally, the kinetics of GB migration at lattice level is discussed. Our work firstly reports the simulation of shock-induced grain boundary migration in iron. It is of great significance to the theory of GB migration and material engineering.

Keywords: shock-loading, grain boundary migration, iron, phase transition

PACS: 62.50.–p, 47.40.Nm **DOI:** 10.1088/1674-1056/ab4f61

1. Introduction

The migration of grain boundary (GB) is an important mechanism to change the internal structure of materials, so it is of great significance to properties of materials. Previous studies have shown that GBs would move under loading conditions, such as heating,[1] tensile,[2] shear,[3–6] surface deformation[7,8] and irradiation,[9] etc. Particularly, molecular dynamics simulations have indicated that some GBs can migrate automatically only in the thermal fluctuation under the free boundary condition.[4] It is very important to study the GB migration under these loading conditions to deepen our understanding of material science theory. The GB migration can be divided into two types: diffusion-based and shear-coupled ones.[2] Diffusion-based GB migration is achieved by atomic jump and driven by free energy difference.[10] Shear-coupled GB migration will not change the position of atoms dramatically and is driven by the shear stress along the GB surface.[11,12] In addition to the above loading conditions, GB migration also occurs under strong shock-loading conditions because strong shock will cause the instantaneous increases of pressure, shear stress and temperature, which can lead to GB migration. The studies of GB migration under shock-loading are still very little. Long *et al.*[13] found that shock-loading would induce migration of GBs in copper, and the GB migration occurs mainly in ATGBs. However, their works only involve the case that the shock direction is parallel to GBs. Moreover, the shock responses of face-centered cubic (FCC) metals (aluminum and copper) are quite different from those of body-centered cubic (BCC) metals (iron).[14–18] The mechanism of GB migration should be different for different lattice types. At present, we are still unclear about the mechanism of GB migration in iron under strong shock-loading.

Due to the significant role of iron in human industrialists and in the earth's core, the behavior of iron under shock-loading has attracted a great deal of attention. A large number of experiments and simulations have been performed to investigate the shock response of iron.[19–26] A series of experiments[27,28] and simulations[10,29–31] have been carried out to study GB migration in iron. However, GB migration in

*Project supported by the Fundamental Research for the Central Universities of China, the National Key Laboratory Project of Shock Wave and Detonation Physics of China, the Science and Technology Foundation of National Key Laboratory of Shock Wave and Detonation Physics of China, the National Key R&D Program of China (Grant No. 2017YFB0202303), the National Natural Science Foundation of China (Grant Nos. 51871094, 51871095, 51571088, NSFC-NSAF U1530151, and U1830138), the Natural Science Foundation of Hunan Province of China (Grant No. 2018JJ2036), and the Science Challenge Project of China (Grant No. TZ2016001).

†Corresponding author. E-mail: jun_chen@iapcm.ac.cn
‡Corresponding author. E-mail: wyuhu@hnu.edu.cn

© 2019 Chinese Physical Society and IOP Publishing Ltd

iron under strong shock-loading has not been simulated. One of the reasons is that there is no suitable potential to simulate the plasticity of iron before phase transformation under shock for a long time. Therefore, it is impossible to perform the simulation related to the plasticity of iron under shock. Until recent years, Gunkelmann *et al.*[32] and our group (Wang *et al.*[15]) made a breakthrough in iron potential, respectively. Wang *et al.* developed the modified analytic embedded-atom method (MAEAM) potential, successfully simulated the plasticity before phase transition under shock, and greatly reduced the proportion of FCC atoms in phase transition products during BCC→hexagonal close-packed lattice (HCP) (a large number of FCC could not be observed in experimental[22]). After the breakthrough of potential, the simulation of iron under shock has more abundant phenomena than before. Another reason is that the stacking fault energy of iron is so high that GB migration cannot be observed easily in the simulation. Therefore, understanding of GB migration in iron under strong shock is almost absent.

Our group has carried out a series of works to study the interaction between GBs and phase transformation under shock-loading.[17,33–35] Gunkelmann *et al.* made a lot of achievements in studying the shock response of polycrystalline iron.[32,36,37] Unfortunately, the phenomenon of GB migration in iron under shock has never been observed in the simulation. Both symmetrical and asymmetrical grain boundaries have important effects on materials.[38–40] In our previous works, only shock response of iron bicrystal with symmetrical GBs is studied. What about asymmetric GBs? This work studys the shock response of asymmetric GBs, and shows the migration of Σ3 [110] ATGB under shock. The special shock response of GB migration is the reason why we choose Σ3 [110] ATGB. However, there are so many ATGBs, and it is difficult to summarize why only a part of ATGBs in iron under shock can migrate at present. Nevertheless, this paper firstly reports the simulation of GB migration in iron under shock-loading, which can fill in the blank of simulation and provide a reference for the experiment. Moreover, this study about the effect of GB migration on phase transition is an important supplement to our previous works about the interaction between GBs and phase transformation under shock-loading. Also, the mechanism of GB migration in iron under shock will attract a lot of attention because of the need of material dynamic damage research. Therefore, we discuss in detail the GB migration in iron bicrystal under shock-loading in this paper, and the interaction between GB migration and phase transformation under shock-loading are also revealed.

2. Method

Non-equilibrium molecular dynamics (NEMD) simulations are performed through the LAMMPS[41] to investigate the migration of Σ3 [110] ATGB in iron bicrystal under shock. The potential used in this paper is MAEAM potential[15] developed by us recently, which has unique advantages in simulating the plastic behavior in iron under strong shock-loading. Figure 1 is a schematic diagram of the bicrystal. The dimensions of the sample along the X, Y and Z directions are 15.78 nm × 15.78 nm × 240.40 nm, the sample contains about 5.09 million atoms. We have tested that the transverse size of the sample is enough to exclude the size effect. In order to obtain the initial stable sample, the sample is equilibrated with an energy minimization using the conjugate gradient method. It is then thermalized in the isothermal-isobaric ensemble (NPT) at zero pressure, and the X, Y, and Z directions satisfy the periodic boundary condition. It is equilibrated with 800 K about 50 ps, then experienced a cooling process from 800 K to ≤10 K for 100 ps. We find that the different initial temperatures (300 K or 10 K) of the sample would not change our conclusion, but lower initial temperature can help to raise the precision in data analysis. We would confirm that the stress and energy near the GB reach the minimum at last. Finally, periodic boundary condition is applied only to the X and Y directions, the sample is equilibrated about 20 ps in the micro-canonical ensemble (NVE). In this way, the final equilibration condition of the sample can be consistent with the shocked condition. Unless specifically stated in this paper, the shock wave sweeps through the sample from left to right along the Z axis. The shock wave is generated using the piston method. The range of piston velocities is from 0.3 km/s to 0.6 km/s. The time step during sample relaxation is 1 fs, and the time step during shock stage of sample is 0.4 fs. The simulation results are visualized by OVITO.[42] Local structure is identified by adaptive neighborhood analysis.[43] The stress is calculated on the basis of virial stress.[44] The statistic of stress tensor is realized by binning analysis.[45]

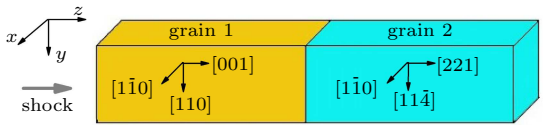


Fig. 1. Schematic configuration of iron bicrystal with asymmetry tilt Σ3 [110] grain boundary. The shock is along the Z direction.

3. Results and discussion

The GB migration in iron under shock has not been observed in previous simulations, where the GBs only provide nucleation sites for phase transformation, and even some GBs can be directly transformed into HCP lattices.[34,35] Due to the fact that the stacking fault energy of iron is very high, the phenomena of dislocation, stacking fault, slip and migration of GB are not easy relatively to be observed in the shock simulation. However, we recently discovered the migration of Σ3 [110] ATGB in iron bicrystal under shock.

3.1. Evidence of GB migration

Phase transformation will be induced during GB migration when the piston velocity is 0.5 km/s. In order to study the interaction between GB migration and phase transition, the results with $u_p = 0.5$ km/s are analyzed emphatically. Figure 2 shows the local morphology of the bicrystal at different times (fixing visible window 70–170 nm along the Z axis) with 0.5 km/s piston velocity. The GB is denoted by the white atoms in the figure, and tends to move to the right. At about 28 ps, phase transition is induced in the region near the left side of the GB during the GB migration. At about 32 ps, the GB is no longer the boundary of two BCC grains, and the left side of the GB is occupied by HCP atoms. Strictly, it can be treated as an interface at this time, but the general interface does not have such a layer of disordered atoms (white atoms). Finally, the HCP phase propagates to the right along with the GB.

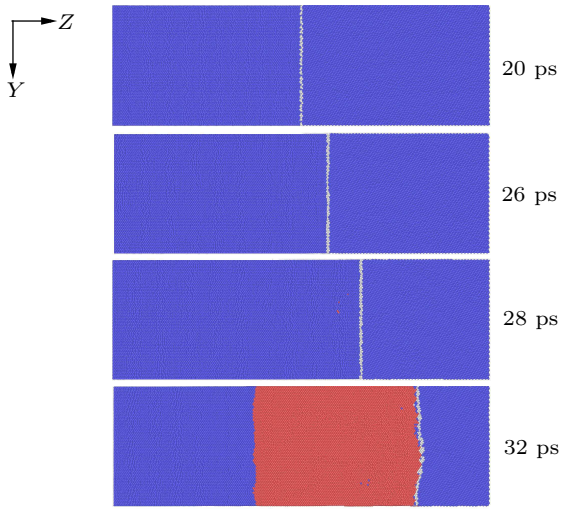


Fig. 2. Atomic microstructure evolution of a shock-loaded iron bicrystal sample containing asymmetry tilt Σ3 [110] grain boundary with the 0.5 km/s piston velocity. The visualization window is fixed at 70–170 nm along the Z axis. Color code: HCP atoms (red), FCC atoms (green), defect atoms denoting the GB atoms (white), and BCC atoms (blue).

Although GB migration can be directly observed in morphology figures at different times, it can also be verified by means of tracing the GB at different times and the original GB atoms. The O in Fig. 3 represents the original GB atoms, while the N represents the new (actual) GB. When the shock wave reaches the GB at about 23–24 ps, the Z coordinate of the N in Fig. 3 begins to increase immediately. Since the shock wave will cause the sample compressed along Z direction, the Z coordinates of atoms will tend to increase slightly and gradually (shock wave is from left to right end). This is why the Z coordinates of O get larger slowly. The Z coordinate of N increases, which indicates that the GB moves to the right. The Z coordinate of O does not change too much, which indicates that there is no jump for atoms, so the GB migration type is shear-coupled.

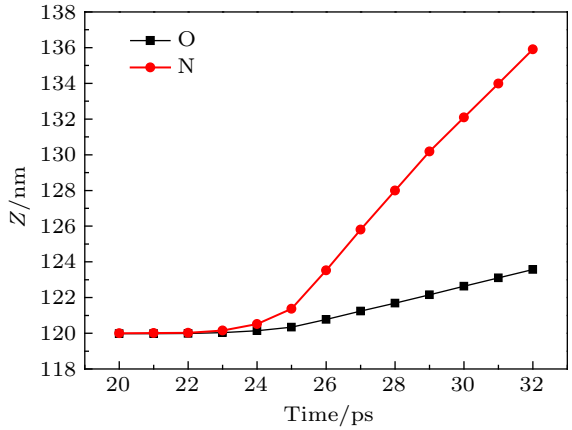


Fig. 3. The evolution of Z coordinates of recorded atoms over time. O represents the average coordinates of the initial grain boundary atoms, and N represents the average coordinates of the grain boundary atoms at each time.

Figure 4 shows the evolution of the shear stress ($\sigma_v = \sigma_{zz} - (\sigma_{xx} + \sigma_{yy})/2$) profile of the shock-loaded sample with $u_p = 0.5$ km/s in the position-time diagrams. The black dashed line represents the location of GB. As shown in Fig. 4, the stress wave reaches the GB at about 23–24 ps, which coincides with the time when the GB begins to migrate in Fig. 3. It is indicated that the GB moves immediately when the shock wave reaches the GB, so the GB migration is very sensitive to the shock wave. The shear stresses on both sides of the GB are different after shock wave sweeps across the GB. The GB migration should be closely related to the difference between shear stresses on both sides of the GB. At about 28 ps, the shear stress on the left side of grain boundary starts to decrease due to the phase transformation.

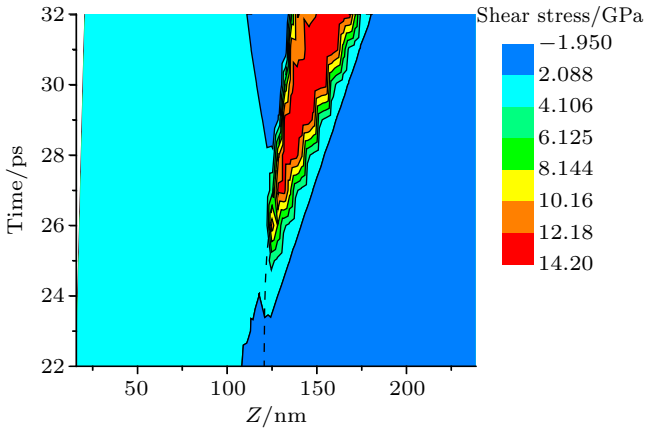


Fig. 4. The position-time-shear stress diagrams for bicrystal shock-loaded with $u_p = 0.5$ km/s. The color coding is based on the shear stress. The black dashed line is the GB position.

3.2. GB migration with different piston velocities

As shown in Fig. 5(a), the GB migration seems to be less sensitive to the initial piston velocity, and the maximum velocities of GB migration with different initial piston velocities are almost the same. Particularly, the velocity of GB migration reaches its maximum value quickly when the piston velocity is 0.6 km/s, then there is a decrease stage. What causes the decrease of GB migration velocity? As shown in Fig. 5(b), the

shock wave (0.6 km/s) could induce the phase transition at the left end of bicrystal, and there is a trough for the velocity profile of the atoms along the Z direction (marked by dashed lines in Fig. 5(b)) before the phase transition wave. The decrease of the velocity wave corresponds to the decrease of the GB migration velocity mentioned above. The velocity of GB migration with the 0.5 km/s piston velocity would also decrease after about 28 ps. The induced phase transition at the same time can be responsible for the decrease (the induced phase transition would reduce the shear stress on the left side of GB in Fig. 4).

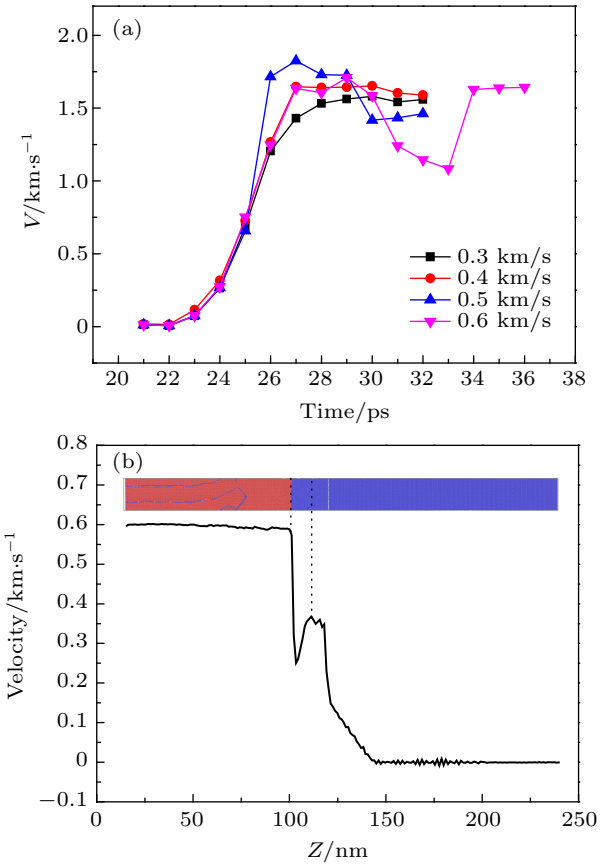


Fig. 5. (a) Evolution of GB migration velocity with different piston velocities. (b) The velocity of atoms along Z direction and the micromorphology of the bicrystal with $u_p = 0.6$ km/s at about 25 ps. The color code is the same as Fig. 2.

3.3. Factors affecting GB migration

It was found that the migration of GB should be related to the shear stress on both sides of GB. Figure 6 shows the variation of the migration velocity of GB and the difference between shear stress on both sides of GB with time. Their change trends are almost the same, which proves that the difference between shear stresses on both sides of the GB has a significant effect on the GB migration. The above simulations correspond to shock waves from left to right. If the shock wave sweeps from right to left, will the GB still migrate? What about the direction of migration? In order to answer the questions, simulations are performed for the case that the shock wave sweeps from right to left with the 0.3 km/s piston velocity. The atoms in the bicrystal tend to move slightly to the left as shown in Fig. 7(a) because of the contrary shock direction (the Z coordination of O decreases gradually), and the GB still moves to the right (the Z coordination of O increases). Additionally, the phase transition also only occur on the left side of the GB when the piston velocity is 0.5. Therefore, the shock direction does not affect the movement direction of GB. Compared with Fig. 4, Fig. 7(b) shows that the shear stress on both sides of GB is different, regardless of the shock direction, and the shear stress on the right side of GB is larger than that on the left side. Therefore, the shock-induced shear stress difference

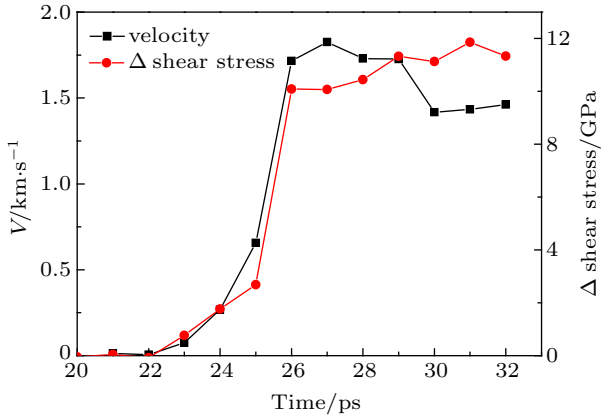


Fig. 6. Evolution of the grain boundary migration velocity and difference between shear stress on both sides of grain boundary with $u_p = 0.5$ km/s.

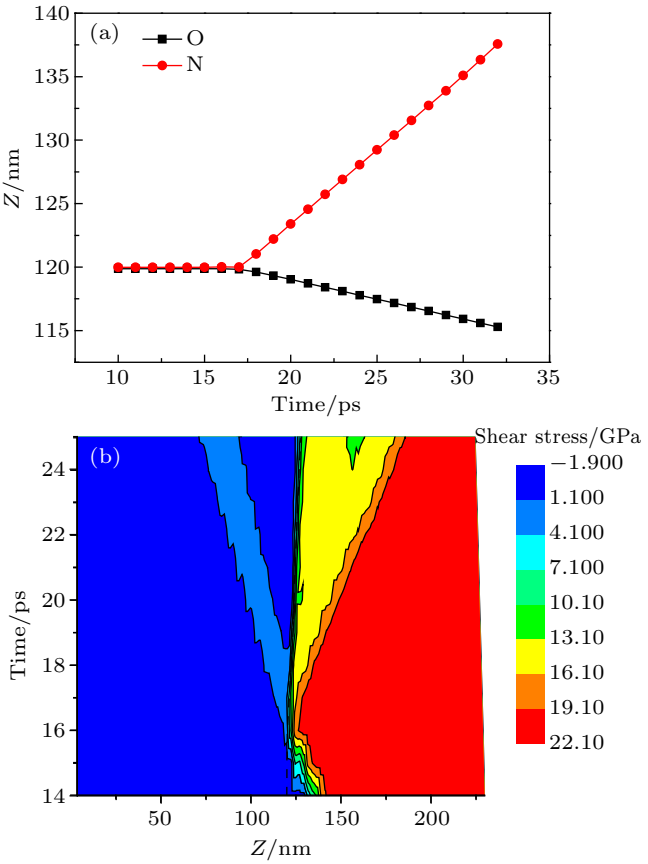


Fig. 7. (a) The evolution of Z coordinates of recorded atoms over time when the shock wave is from right to left and $u_p = 0.3$ km/s. O and N are the same as Fig. 3. (b) The position–time–shear stress diagrams of bicrystal, where the color coding is based on the shear stress.

between both sides of GB is an important factor leading to GB migration. The difference of lattice orientation on both sides of GB is the reason for the difference of shear stress on both sides of GB under shock, while one of characteristics of ATGBs is that the lattice orientations on both sides of GB are different. This can explain the conclusion of Long *et al.* that migration of GBs occurs mainly in ATGBs.[13]

As mentioned above, the GB migration begins between about 23 and 24 ps when the piston velocity is 0.5 km/s. In Fig. 8, there is almost no difference between the configurations of the GB at 26 ps and the original GB (they are both the planes). This indicates that there is no deformation of GB or change of local configuration during GB migration. Due to the appearance of phase transformation near the GB, the uniform propagation of the GB is broken, and the deformation of the GB is induced (see Fig. 8). That is to say, the inhomogeneous growth of HCP phase would lead to the deformation of the GB.

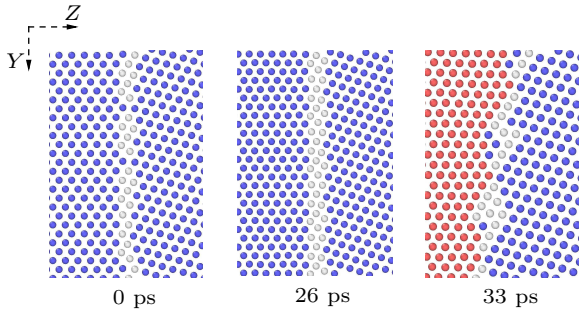


Fig. 8. Local atomic configuration near the GB selected at different times with $u_p = 0.5$ km/s, where the color code is the same as Fig. 2.

3.4. Dynamics of GB migration

The study of dynamics can help to reveal the mechanism of GB migration. Figure 9 shows a group of atoms at different times near the right of GB with $u_p = 0.5$ km/s. Atoms 4, 5, and 6 are on the same layer (first layer), while other atoms belong to another layer (second layer). The color code is the same as Fig. 2. Figure 9(b) shows that the GB moves here at about 25 ps. At that moment, the BCC lattice is converted to the GB (Figs. 9(b) and 9(c). At about 25.6 ps (Fig. 9(d)), the atoms are rearranged according to BCC lattice after leaving of the GB. For the second layer atoms, we use atomic 1 as a reference system, atoms 2, 3, 7, and 8 move along the $[11\bar{1}]_{G2}$ direction, others hardly move. Although both figures 9(a) and 9(d) correspond to the BCC lattice, the orientation relationship between them is inconsistent. Figures 9(a)–9(d) are equivalent to the original BCC lattice rotating at an angle with fixing the X axis (in addition, figure 9(d) is compressed BCC lattice under shock). At about 29.2 ps (Fig. 9(f)), the new BCC is converted into HCP. The difference between Figs. 9(d) and 9(f) seems that only the first layer atoms move a little along the Y axis. Because this region is very close to the GB, the phase transition has not been induced when the GB moves here, so the transformation process is original BCC lattice→GB→new BCC lattice→HCP lattice.

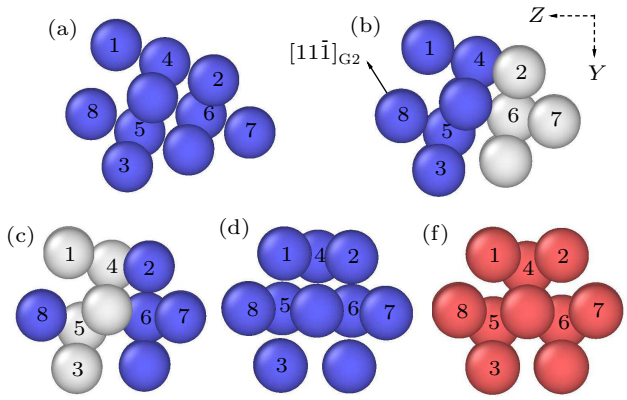


Fig. 9. A group of atoms near the right side of the grain boundary with $u_p = 0.5$ km/s at different times: (a) 0 ps, (b) 25 ps, (c) 25.2 ps, (d) 25.6 ps, (f) 29.2 ps. The color code is the same as Fig. 2. G2 means grain 2.

Figure 10 shows a group of atoms at about 10 nm away from the right side of GB at different times with $u_p = 0.5$ km/s. Because it is far away from the GB, the HCP phase on the left side of the GB has grown up when the GB moves to this region. Therefore, in Figs. 10(b) and 10(c), there are not only white atoms representing the GB, but also red atoms representing HCP. And there is no new BCC lattice that has been formed. Finally, the GB propagates with the phase transition (see Fig. 2), so the transformation is: BCC lattice→GB→HCP lattice.

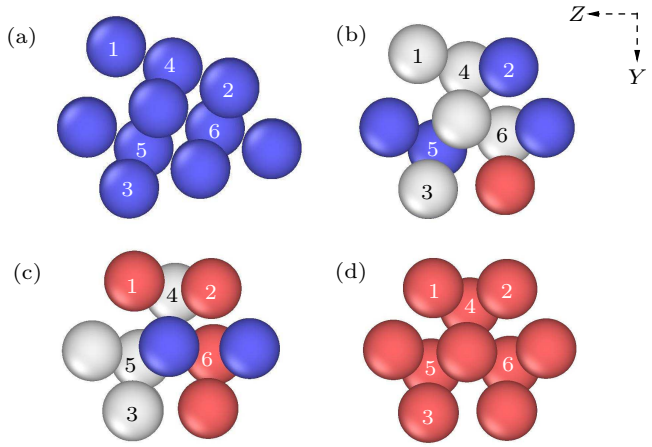


Fig. 10. A group of atoms at about 10 nm to the right of the GB with $u_p = 0.5$ km/s at different times: (a) 0 ps, (b) 29.6 ps, (c) 29.8 ps, (d) 30.2 ps. The color code is the same as Fig. 2.

In order to investigate the mechanism of GB migration, we would track the movement of the selected atoms. Lattice constants are defined in the legend of Fig. 11. As shown in Fig. 11(a), a decreases slightly at 23–24 ps, which corresponds to the lattice compression along the Z direction because the reach of shock wave (the connection of atoms 1 and 2 is approximately in the same direction as the Z axis, so a is very sensitive to the compression caused by the shock wave). At 24–26 ps, a decreases to about 0.6, b decreases to about

0.85, and r increases to 1. It is exactly the process of BCC lattice→GB→new BCC lattice (the distance between atoms 5 and 3 is exactly the same as that between atoms 1 and 3 in Fig. 9(d), which corresponds to $r = 1$). Then, r decreases to about 0.75 at 29 ps, corresponding to BCC→HCP transition. At the same time, there is no change for a and b, indicating that there is only slip (as mentioned above, the first layer atoms move a little along the Y axis in Figs. 9(d)–9(f), there is no change in the distances between atoms in the same layer). It is well known that the BCC→HCP transition can be divided into two stages: compression and slip. However, there is only slip stage in the phase transition here, which indicates that the lattice has been compressed to satisfy the requirement of phase transition (it is enough for a reducing to about 0.6) during the GB migration. Therefore, the lattice compression along the Z axis (decrease of a) caused by GB migration can help to trigger the slip to induce the phase transition. This can explain why the phase transition only takes place on the left side of the GB. However, the assistance of GB migration seems to be limited, because the phase transition threshold of the sample is not much lower than that of the single crystal. Figure 11(b) is associated with Fig. 10. Unlike Fig. 11(a), r would not increase to 1 (instead increase directly to 0.75), it corresponds to the transformation in Fig. 10: BCC lattice→GB→HCP lattice. Therefore, the dynamics of GB migration can be affected by the phase transformation.

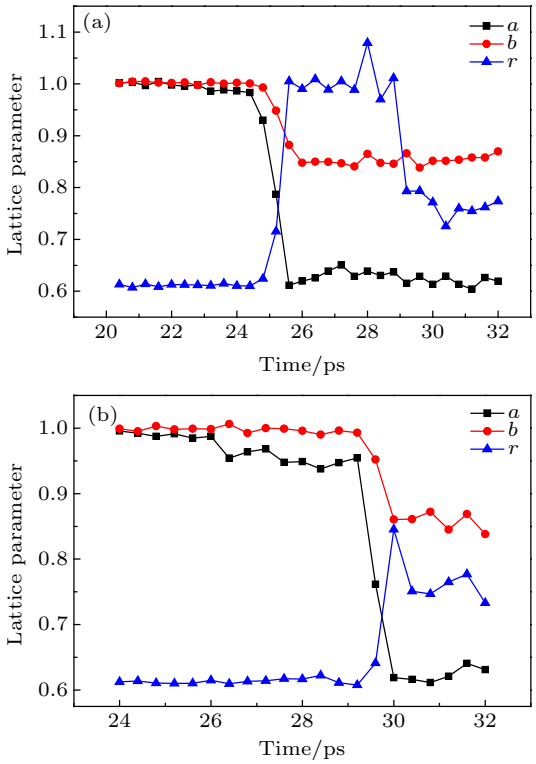


Fig. 11. The change of lattice parameters with time when $u_p = 0.5$ km/s. The definition of lattice parameters a, b, r corresponds to Fig. 9(a) and Fig. 10(b). Here a is the distance between atoms 1 and 2, b is the distance between atoms 1 and 3, c is the distance between atoms 3 and 5, d is the distance between atoms 1 and 5, and r is the ratio of c to d. The lattice parameters a and b are scaled.

It has been mentioned above that GB migration is beneficial to phase transition, but it does not seem to have much effect on the threshold of phase transition. Figure 12 shows the evolution of lattice parameters of a group of atoms near the right side of GB (the same atoms in Fig. 9) with piston velocity 0.3 km/s. The definitions of parameters are the same as Fig. 11. There is no phase transition in the bicrystal, so the transformation near the right side of the GB is: BCC lattice→GB→BCC lattice. The changes of a, b, and r in Fig. 12 are similar to those in Fig. 11(a) before 28 ps. However, a decreases to about 0.65 instead of 0.6, because the lattice compression with 0.3 km/s is smaller than that with 0.5 km/s. The degree of lattice compression does not satisfy the need of slip, so there is no phase transition in the sample.

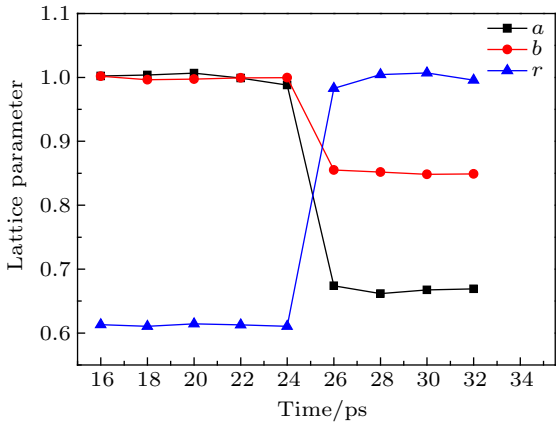


Fig. 12. The variation of lattice parameters of atoms in Fig. 9 with time when $u_p = 0.3$ km/s. The definitions of a, b, and r are the same as those in Fig. 11.

4. Conclusions

We have investigated the shock-induced migration of Σ3 [110] ATGB in α iron bicrystal via NEMD simulations. We observe the Σ3 [110] ATGB migration in iron bicrystal under shock and the migration type is shear-coupled. The shock-induced migration of Σ3 [110] ATGB would not change the shapes and local structures of GBs without the effect of phase transition. The migration of GBs seems to be less sensitive to the piston velocity, and the maximum velocities of GB migration with different piston velocities between 0.3 km/s and 0.6 km/s are nearly the same. The shock-induced shear stress difference between the two sides of GB is the key factor leading to GB migration, which can explain why migration of GBs occurs mainly in ATGBs. In particular, the dynamics of GB migration in iron is revealed firstly, and GB migration can help induce the phase transition. Also, it has been found that the phase transformation near the GB would change the shape and migration mechanism of GBs.

Acknowledgment

The authors would like to acknowledge the support of the computation platform of the National Super-Computer Center

in Changsha (NSCC).

References

[1] Li Y H, Wang L, Li B, E J C, Zhao F P, Zhu J and Luo S N 2015 *J. Chem. Phys.* **142** 054706
[2] Legros M, Gianola D S and Hemker K J 2008 *Acta Mater.* **56** 3380
[3] Rajabzadeh A, Mompiou F, Legros M and Combe N 2013 *Phys. Rev. Lett.* **110** 265507
[4] Cahn J W, Mishin Y and Suzuki A 2006 *Acta Mater.* **54** 4953
[5] Winning M, Gottstein G and Shvindlerman L S 2001 *Acta Mater.* **49** 211
[6] Winning M, Gottstein G and Shvindlerman L S 2002 *Acta Mater.* **50** 353
[7] Zhang H, Upmanyu M and Srolovitz D J 2005 *Acta Mater.* **53** 79
[8] Sursaeva V G, Straumal B B, Gornakova A S, Shvindlerman L S and Gottstein G 2008 *Acta Mater.* **56** 2728
[9] Li N, Wang J, Wang Y Q, Serruys Y, Nastasi M and Misra A 2013 *J. Appl. Phys.* **113** 023508
[10] Holm E A and Foiles S M 2010 *Science* **328** 1138
[11] Trautt Z T, Adl, A, Karma A and Mishin Y 2012 *Acta Mater.* **60** 6528
[12] Molodov D A, Gorkaya T and Gottstein G 2011 *J. Mater. Sci.* **46** 4318
[13] Long X J, Wang L, Li B, Zhu J and Luo S N 2017 *J. Appl. Phys.* **121** 045904
[14] Bisht A, Ray N, Jagadeesh G and Suwas S 2017 *J. Mater. Res.* **32** 1484
[15] Wang K, Xiao S, Deng H, Zhu W and Hu W 2014 *Int. J. Plast.* **59** 180
[16] Ma W, Zhu W and Jing F 2010 *Appl. Phys. Lett.* **97** 121903
[17] Wang K, Zhu W, Xiao S, Chen K, Deng H and Hu W 2015 *Int. J. Plast.* **71** 218
[18] Amadou N, de Resseguier T, Dragon A and Brambrink E 2018 *Phys. Rev. B* **98**
[19] Bancroft D, Peterson E L and Minshall S 1956 *J. Appl. Phys.* **27** 291
[20] Yaakobi B, Boehly T R, Meyerhofer D D, Collins T J B, Remington B A, Allen P G, Pollaine S M, Lorenzana H E and Eggert J H 2005 *Phys. Rev. Lett.* **95** 075501
[21] Kalantar D H, Belak J F, Collins G W, Colvin J D, Davies H M, Eggert J H, Germann T C, Hawreliak J, Holian B L and Kadau K 2005 *Phys. Rev. Lett.* **95** 075502
[22] Hawreliak J, Colvin J D, Eggert J H, Kalantar D H, Lorenzana H E, St, Ouml J S, lken, Davies H M, Germann T C and Holian B L 2006 *Phys. Rev. B* **74** 184107
[23] Kadau K, Germann T C, Lomdahl P S and Holian B L 2005 *Phys. Rev. B* **72** 064120
[24] Chen Z, Ding J, Zhou F, Tang C, Ye Z and Wu X 1988 *Chin. Phys. Lett.* **5** 313
[25] Li J, Wu Q, Yu J D, Tan Y, Yao S L, Xue T and Jing K 2017 *Acta Phys. Sin.* **66** 146201 (in Chinese)
[26] Ma W, Zhu W J, Zhang Y L and Jing F Q 2011 *Acta Phys. Sin.* **60** 066404 (in Chinese)
[27] Tsurekawa S, Ueda T, Ichikawa K, Nakashima H, Yoshitomi Y and Yoshinaga H 1996 *Mater. Sci. Forum* **204-206** 221
[28] Yu Z S and Shewmon P G 1982 *Metall. Trans. A* **13** 1567
[29] Wejrzanowski T, Spychalski M, Pielaszek R and Kurzydlowski K J 2007 *Solid State Phenom.* **129** 145
[30] Teus S M, Mazanko V F, Olive J M and Gavriljuk V G 2014 *Acta Mater.* **69** 105
[31] Jian Y, Yi W, Yan X, Hou H and Jing T W 2018 *Comput. Mater. Sci.* **148** 141
[32] Gunkelmann N, Bringa E M, Kang K, Ackl, G J, Ruestes C J and Urbassek H M 2012 *Phys. Rev. B* **86** 144111
[33] Wang K, Chen J, Zhang X and Zhu W 2017 *J. Appl. Phys.* **122** 105107
[34] Zhang X, Wang K, Zhu W, Chen J, Cai M, Xiao S, Deng H and Hu W 2018 *J. Appl. Phys.* **123** 045105
[35] Zhang X Y, Chen J, Hu W Y, Zhu W J, Xiao S F, Deng H Q and Cai M Q 2019 *J. Appl. Phys.* **126** 045901
[36] Gunkelmann N, Bringa E M, Tramontina D R, Ruestes C J, Suggit M J, Higginbotham A, Wark J S and Urbassek H M 2014 *Phys. Rev. B* **89** 140102
[37] Gunkelmann N, Tramontina D R, Bringa E M and Urbassek H M 2014 *New J. Phys.* **16** 093032
[38] Luo S N, Germann T C, Tonks D L and An Q 2010 *J. Appl. Phys.* **108** 093526
[39] Hahn E N, Fensin S J, Germann T C and Meyers M A 2016 *Scr. Mater.* **116** 108
[40] Zong H X, Ding X D, Lookman T and Sun J 2016 *Acta Mater.* **115** 1
[41] Plimpton S 1995 *Comput. Mater. Sci.* **4** 361
[42] Stukowski A 2010 *Model. Simul. Mater. Sc.* **18** 015012
[43] Stukowski A 2012 *Model. Simul. Mater. Sc.* **20** 45021
[44] Thompson A P, Plimpton S J and Mattson W 2009 *J. Chem. Phys.* **131** 154107
[45] Luo S N, An Q, Germann T C and Han L B 2009 *J. Appl. Phys.* **106** 013502